Golden Age of Fluorenylidene Phosphaalkenes—Synthesis, Structures, and Optical Properties of Heteroaromatic Derivatives and Their Gold Complexes

Joshua P. Green, Daniel Morales Salazar, Arvind Kumar Gupta, and Andreas Orthaber*

Cite This: *J. Org. Chem.* 2020, 85, 14619−14626

Read Online

ACCESS | Metrics & More | Article Recommendations | SI Supporting Information

ABSTRACT: The substitution of 2,7-dibromo-9-fluorenyl phosphaalkenes with heteroaromatic substituents (bithiophene, benzothiophene, pyridine) offers access to interesting push−pull dye molecules. Steric shielding due to the bulky P-substituent gives marked different reactivities at the 2- and 7-positions, allowing the synthesis of mixed/asymmetric derivatives. Further functionalization via gold(I) coordination was demonstrated and increased the acceptor character, concomitant with a red-shifted absorption.
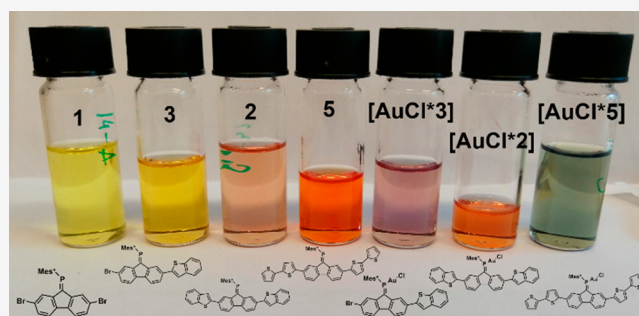
INTRODUCTION

The construction of extended π-conjugated frameworks can be rationally based on the combination of different conjugated aromatic building blocks.[1,2] The combination of suitable donor and acceptor units often leads to interesting optical and electronic properties.[3,4] For example, 9,9-dialkylated fluorene derivatives (Figure 1, **I**) have been used extensively as efficient
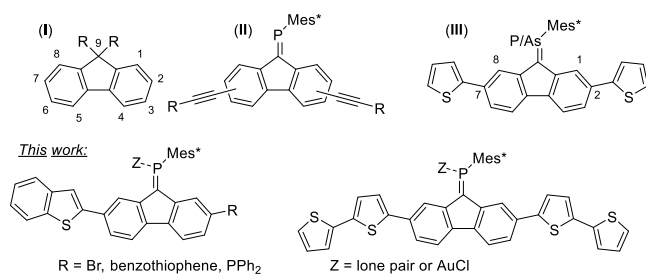

Figure 1. Molecular fluorene derivatives, including the numbering scheme used herein (top, **I** and **III**) as well as various phospha/arsaalkene derivatives.

π-spacers in the construction of photoluminescent materials, dyes for dye-sensitized solar cells, and other optoelectronic applications.[5−11] The dialkylation significantly enhances solubility and has an influence on molecular packing, e.g., π-stacking; however, it does not significantly alter the optical and electronic properties compared to the parent 2H-fluorene.[12] Similarly, dibenzoheteroles of group 14 to 16 have found widespread use as optoelectronic materials.[13−18] Fluorene cores can also be functionalized with thiophene or benzothiophene moieties to provide diverse optoelectronic

properties such as solvatochromism, tunable emission, etc.[19−23]

The incorporation of main group elements into π-conjugated materials has been identified as a promising path to new functional materials with outstanding optoelectronic properties.[24−27] In particular, phosphorus has led to a number of interesting optoelectronic materials that exploit its variable bonding situations and coordination modes.[28] Over the past years, our group has been interested in utilizing the fluorene core as a strong acceptor unit by introducing supermesitylphosphinidene or -arsinidene fragments (Mes*-P: or Mes*-As:, where Mes* = 2,4,6-tri-*tert*-butyl phenyl) at the bridgehead position (Figure 1, **II** and **III**).[29] This sterically demanding substituent greatly affects solubility and the solid-state packing of these materials, and the possible metal coordination is expected to have similar effects. Notably, the steric demand of the Mes* substituent also has a remarkable effect on the reactivity and electronic situation of the two sides of the molecule, as reflected in the low and high NMR frequencies of protons in the 1- and 8-positions of such compounds, respectively.[30,31]

Herein, we describe the synthesis of novel thiophene and benzothiophene derivatives using Stille coupling of the parent 2,7-dibromo-fluorenylidene phosphaalkene and suitable stann-

yl derivatives. The different environments at the 2- and 7-positions caused by the steric demand of the Mes* substituent allow for selective monofunctionalization at the less hindered position, while difunctionalization requires harsher reaction conditions. Solid-state structures of these derivatives are reported, together with optical characterizations and theoretical studies of these products.

■ RESULTS AND DISCUSSION

The common precursor for the target molecules was the 2,7-dibromo-fluorenyl phosphaalkene (**1**). Initially we attempted the derivatization of this building block using Suzuki-type coupling protocols; however, the tested conditions did not result in C−C coupling and/or were incompatible with the phosphaalkene moiety, mostly leading to degradation products of the P═C bond, for example, by the formation of the corresponding (partially) brominated fluorenyl ketone and the Mes*-phosphinic acid.[32] Thus, milder coupling conditions were required. Stille coupling protocols often perform well at moderately elevated temperatures and do not require additional components such as inorganic bases (Scheme 1). First,

**Scheme 1. Synthesis of Fluorenyl Phosphaalkene Derivatives Using Stille Coupling Reactions**[a]
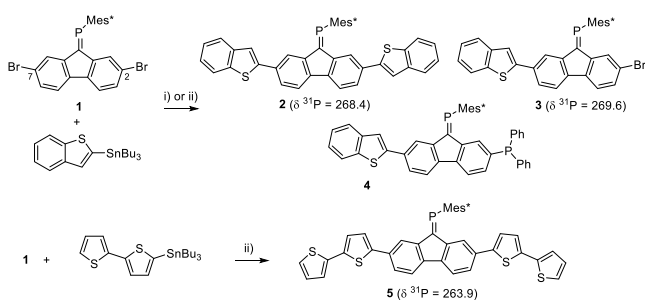
[a](i) THF, [Pd(PPh₃)₄], μw 60 min 120 °C. (ii) THF, [Pd(PPh₃)₄], μw 45 min 120 °C.

we attempted the synthesis of the 2,7-di(2-benzo[b]-thiophene) derivative **2** by conventional and microwave heating using [Pd(PPh₃)₄] as a catalyst. Despite an excess of the stannyl reagent, analysis of the ^{31}P-spectra of the crude reaction mixture indicated formation of a variety of different species containing phosphorus centers in both the phosphaalkene and phosphine region. Chromatographic workup afforded the targeted disubstituted derivative in 5% isolated yield. The ^{31}P-resonance at 268.4 ppm is in the expected range for this compound and is indicative of a normally polarized fluorenyl phosphaalkene. Despite the isolation of **2** in low yield, all reaction conditions tested gave the monosubstituted product **3** as the major product. The presence of a single isomer of **3** was confirmed by NMR spectroscopy, with a single ^{31}P resonance at 269.6 ppm and one set of proton/carbon signals being detected. This behavior can be rationalized by the different environments at the fluorenyl core introduced by the phosphaalkene moiety and the steric demand of the Mes* substituent, which shields the C2−Br group significantly and reduces its reactivity. The spatial proximity of the Mes* group is also reflected in the low-frequency resonance of proton H1 due to the ring current effect, with the observed shift being 5.43 ppm.

Further attempts to increase formation of **2** using harsher reaction conditions such as increased reaction time and

temperature led to the formation of another derivative, which upon separation via chromatography could be identified by selective crystallization from several fractions as the 2-diphenylphosphine-7-benzothiophene derivative **4**. Due to the small quantities of this side product, only single crystal analysis could be performed. The PPh₂ fragment could originate from Ph₂P−C₆H₅ cleavage of a triphenylphosphine ligand in the catalytically active palladium $[Pd(PPh_3)_n]$ species, which could interfere with the productive transmetalation step.[33,34] This is particularly plausible due to the large SnBu₃ stannyl groups at the sterically shielded 2-position of the thiophene/benzothiophene reagents. We also attempted coupling of bithiophene to **1**, encountering similar difficulties. Nonetheless, we were able to obtain the targeted disubstituted product **5** in ca. 15% yield using a microwave Stille coupling protocol (see details in the Experimental Section). Similar behavior was also observed in the attempted coupling of thiophene (using C₄SH₄−SnBu₃), which predominantly afforded the monosubstituted derivative **6** (for details see the SI). Further attempts to couple other heteroaromatic units proved similarly difficult (Scheme 2).

**Scheme 2. Coupling Reactions of 1 with 2-Stannyl Pyridine**[a]
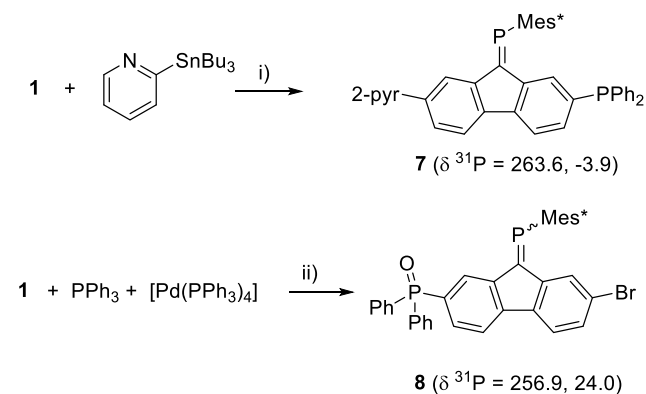
[a](i) THF, [Pd(PPh₃)₄], μw 45 min, 140 °C and in the absence of a stannyl reagent. (ii) THF, μw 90 min, 165 °C.

The coupling of **1** with 2-tributylstannylpyridine using similar conditions as before gave the mixed pyridyl/diphenylphosphine derivative **7** as the only isolated product in 10% yield. In order to investigate this reactivity, we reacted **1** with [Pd(PPh₃)₄] and excess triphenylphosphine under microwave heating in THF. From the crude reaction mixture, we identified residual starting material **1** (δ ^{31}P = 272.7 ppm), a mixture of the two monobromo derivatives (7-bromo-fluorenylidene phosphaalkene and 2-bromo-fluorenylidene phosphaalkene, δ ^{31}P = 268.9 and 264.0 ppm, respectively; see SI Figure 19),[30] and a phosphaalkene species in which the ^{31}P peak had shifted to lower frequencies (δ ^{31}P = 255.2 ppm). Chromatographic workup allowed us to identify this compound as the 7-diphenylphosphine oxide-2-bromo-fluorenyl phosphaalkene **8**. Preliminary work using Ph₂P(TMS) as diphenylphoshine source gave promising results, which will be subject of future work.[35] We assume that oxidation of the phosphine was either a result of traces of water/hydroxide under these harsh reaction conditions[36] or took place during workup.

Having sufficient quantities of **2**, **3**, and **5** on hand, we also tested their behavior as ligands toward Au(I). A dichloromethane solution of the respective phosphaalkene was reacted

at room temperature with a solution of [AuCl(*tht*)] (*tht* = tetrahydrothiophene) to give the corresponding gold chloride complex quantitatively upon removal of all volatiles (Scheme 3). Immediate reaction can also be judged by the intense color

Scheme 3. Gold(I) Coordination of Derivatives 2, 3, and 5[a]

2: R^1 = R^2 = 2-benzothiophene
3: R^1 = 2-benzothiophene, R^2 = Br
5: R^1 = R^2 = 2-bithiophene
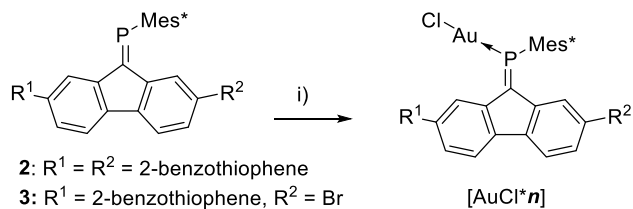
[a](i) DCM, r.t., 2 h.

change, i.e., red-shifted absorption, upon addition of the gold(I) solution. Complex [AuCl*3] showed a ^{31}P NMR resonance of 182.4 ppm, which corresponds to a coordination shift ($\Delta\delta$ ^{31}P) of −87.2 ppm and is indicative of a strong Au−P interaction.[37−39] Notably, the proton in proximity to the Au center was shifted to higher frequencies (9.91 ppm compared to 8.58 ppm), while the proton at position-1, which was directly positioned in the ring current of the Mes* substituent, was shifted further to lower frequencies (5.27 ppm compared to 5.43 ppm). The corresponding disubstituted derivative **2** showed similar behavior upon complexation to gold(I). A coordination shift of $\Delta\delta$ ^{31}P = −87.0 ppm and a high frequency proton shift to 9.93 ppm (compared to 8.63 ppm in **2**) indicate similar AuCl coordination. The gold(I) complex of **5** was characterized by a coordination shift of $\Delta\delta$ ^{31}P = −84.3 ppm, which was the smallest shift observed among this series. The diagnostic shielded aromatic proton was only slightly more shielded (from 6.31 to 6.23 ppm), while the high-frequency proton was more significantly affected (from 8.47 to 9.74 ppm).

Crystallographic and Spectroscopic Characterization. Compound **2** crystallized in the monoclinic space group $P2_1/c$ as dark red needles. The molecule showed disorder in the unhindered benzothiophene, with S2A/S2B having 0.58:0.42 occupancy (Figure 2). On the other hand, the sterically shielded benzothiophene containing S1 showed no signs of disorder. The former was almost coplanar with the fluorene moiety (twist angle 1.9(2)°), while the latter was significantly distorted from coplanarity (24.1(1)°). The P=C bond was 1.691(3) Å, and the C−P=C angle of 106.7(1)° was in the expected range for these compounds (147 CP=C fragments mean P=C distance and C−P=C angle 1.689 Å and 103.7°).[40−42] The difference in steric demand is also reflected in the P−C1−C*n* angles, which were 119.0(2)° and 135.6(2)° toward C2 and C5, respectively. The extended π-conjugated system led to interesting stacking in the solid state, with slipped π−π stacking roughly positioning a benzothiophene unit above the fluorenyl phosphaalkene π-system. One short centroid−centroid distance of 3.77 Å and several slightly longer ones (>4.2 Å) can be calculated.

Compound **3** crystallized as dark orange needles in the orthorhombic space group *Pcnn* with two independent molecules in the asymmetric unit, one of which showed benzothiophene disorder (0.86:0.14), as well as the *para-tert*-butyl group. The solid-state structure confirmed the presence of the expected isomer that had the benzothiophene at the
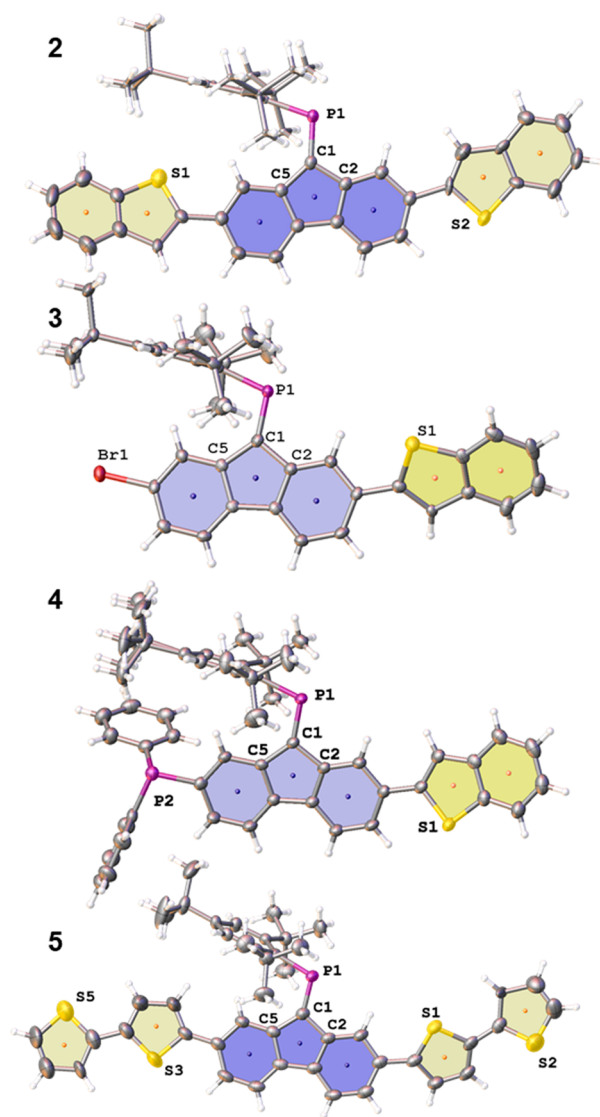

Figure 2. ORTEP-type representations of the solid-state structure of compounds **2−5** (ellipsoid probability level 50%). Colored centroids are placed in the planes. Further details of the structure solutions can be found in the SI.

exposed position, while the bromide substituent remained in the sterically shielded position. The bond metrics were very similar to those found in **2**, with a P=C distance of 1.685(4) Å and a slightly smaller C−P−C angle of 104.0(2)°. The P=C−C*n* angles were 118.3(3)° and 136.3(3)° toward C2 and C5, respectively, illustrating this asymmetry.[43] The π-stacking was weaker in this molecule, with only one noticeable centroid−centroid distance of 3.94 Å.

The phosphine/phosphaalkene **4** had a typical phosphaalkene environment (P=C 1.692(3) Å, C−P=C 105.6(1)°), and near coplanarity between the fluorenyl and benzothiophene was observed, with a twist angle of 8.6(1)° between the two least-squares planes. The diphenylphosphine moiety was rotated away from the Mes* unit, minimizing steric congestion, but otherwise had typical metrics, such as P−C single bond distances of ca. 1.83 Å. The dibithiophene derivative **5** crystallized as dark red blocks in the triclinic space group $P\bar{1}$ containing four independent molecules and a solvent (DCM) in the unit cell. Most thiophene moieties—but, in particular, the terminal thienyl units—were disordered, and significantly

lower coplanarity was seen compared to the benzothiophene derivatives. This illustrates the rotational freedom of the bithiophene substituents over the restricted benzannulated thiophene. The phosphaalkene moieties were all within the expected range of P=C distances (1.675−1.685 Å), and the other metrics were comparable to the other derivatives discussed herein.

Obtaining the single crystal solid-state structures of [AuCl*2] and [AuCl*3] also allowed us to study the impact of gold coordination on the bond metrics and packing in the solid state (Figure 3). Complex [AuCl*2] also crystallized in
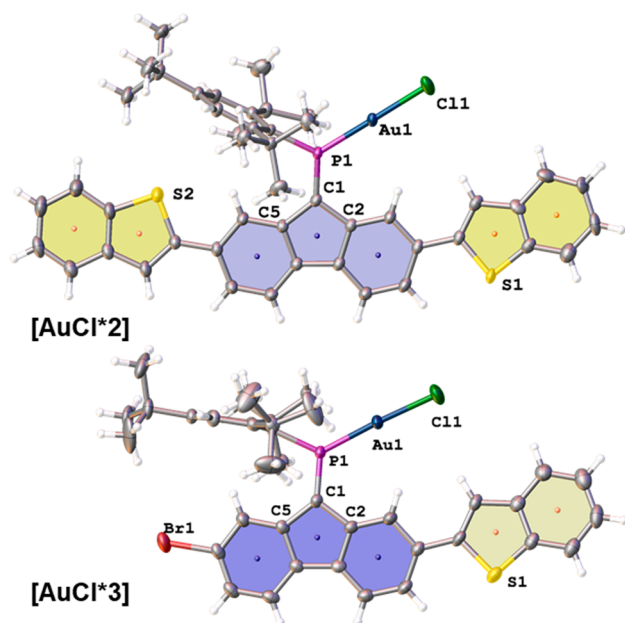

Figure 3. ORTEP-type representations (50% ellipsoid probabilities) of the solid-state structures of gold complexes [AuCl*2] and [AuCl*3]. Colored centroids are placed in the planes.

the monoclinic space group $P2_1/c$ as dark bluish-green needles. The P=C bond was significantly shortened (1.672(3) Å) compared to **2**, while the C−P=C angle became wider (114.3(1)°) as expected upon gold coordination;[44] the P−C1−Cn angles fell into the expected range (C5 = 130.6(2)° and C2 = 123.5(2)°). The AuCl fragment was linear, and the P−Au distance was 2.222(1) Å, which is typical of phosphaalkene gold complexes.[45,46] Overall, the molecular packing was very similar to that of **2**; however, the intramolecular interactions showed increased π−π interactions in [AuCl*2], with centroid−centroid distances in the range of 3.7−3.9 Å (**2**: 3.7−4.3 Å). The benzothiophene moiety containing S1/S1B showed positional disorder with 0.63:0.37 occupancy. All benzothiophene substituents were nearly coplanar with the central fluorenyl π-system, with torsion angles between the planes being <10°. Similarly, the metal coordination in [AuCl*3] resulted in short P=C (1.675(6) Å) and Au−P (2.217(1) Å) distances, as well as a slightly widened C−P=C angle (110.8(3)°). The P−C1−Cn angles were 110.8(3)° and 131.5(4)° for n = 2 and 5, respectively, with these values being somewhat smaller for the former and very similar for the latter compared to the complex [AuCl*2]. Intramolecular interactions were affected by the incorporation of a solvent molecule (DCM) into the unit cell, which resulted in CH-π interactions (H-centroid distances of 2.988 Å) and

weak π−π interactions (centroid−centroid distances of 3.928 and 4.131 Å).

Substitution of the fluorenyl phosphaalkene with (benzo-)thiophenes had a profound impact on the UV−vis absorption properties (Figure 4). While the parent dibromo-derivative **1**
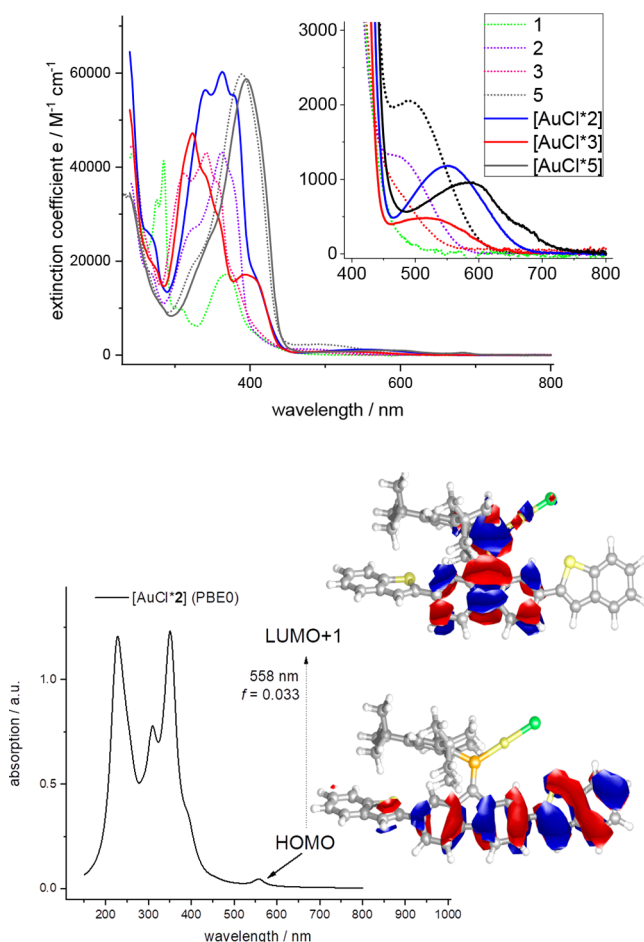

Figure 4. (Top) Experimental optical spectra of compounds **2**, **3**, **5**, [AuCl*2], [AuCl*3], and [AuCl*5] in DCM. (Bottom) An illustrative example of modeled optical transitions of [AuCl*2] using the TD-DFT M06-2X/6-311G**(LANL2DZ)//PBE1PBE/6-31++G**(LANL2DZ) level of theory. The indicated low energy transition corresponds mainly to a HOMO (extended π-fluorenyldibithiophene) to LUMO+1 (heterofulvenoid π*) transition.

appeared yellow, with the lowest energy absorption peak being at 369 nm (λ_{onset} ca. 480 nm), these new derivatives had clearly red-shifted absorption onsets/maxima. The mono- and disubstituted derivatives **3** and **2** had very similar low energy absorptions features, with a shoulder at 486 nm and λ_{onset} ca. 575 nm; however, the extinction coefficient of this feature in **2** was almost double that of the same band in **3** (see inset in Figure 4-top, ε = 1200 and 680 dm³ mol⁻¹ cm⁻¹, respectively). The main absorption bands in the UV had similar structures but were red-shifted for **2** (λ_{max} = 362 nm) compared to **3** (λ_{max} = 341 nm). Interestingly, the dibithiophene derivative **5** showed the most red-shifted onset of absorption (620 nm) and low energy absorption peak (shoulder at 494 nm, ε = 2050 dm³ mol⁻¹ cm⁻¹) as well as strong bands (λ_{max} = 389 nm). Gold(I) coordination increased the acceptor properties of the phosphaalkene moiety (see below), which is clearly reflected in the further red-shift of the maximum absorption bands.

Complexes [AuCl*3], [AuCl*2], and [AuCl*5] have their lowest energy absorption maxima at 518, 533, and 587 nm, respectively, corresponding to red-shifts of 32, 47, and 97 nm, respectively. While the solubility of the free phosphaalkenes was good to excellent in organic solvents such as benzene, DCM, and chloroform, the solubility of the corresponding gold complexes of **2** and **3** dropped by at least a factor of five (0.5 and 0.2 mM in DCM, respectively). In contrast, [AuCl*5] had a solubility of ≫2 mM, suggesting that the rotational freedom of the thienyl units (cf. also disorder in the solid-state structure) had a positive impact on the solubility.

An illustrative example of the observed low energy optical transition is shown for [AuCl*2], with a calculated transition energy of 558 nm (obs. 533 nm) composed mainly of a HOMO to LUMO+1 transition. The HOMO is mainly composed of the conjugated benzothiophene and fluorenyl π orbitals, while the LUMO+1 exhibits a π* character localized on the phosphaalkene fluorenyl core. This also underlines the importance of lone pair modifications such as coordination of gold(I) chloride on the low energy transitions, with this resulting in increased acceptor character leading to the observed red-shifted maxima.

In summary, we have demonstrated the functionalization of fluorenyl phosphaalkenes using heteroaromatic stannyl reagents. The steric shielding provided by the Mes* substituent led to distinctively different reactivities for the C2−Br and C7−Br sites, allowing us to introduce a strong asymmetry into the system. Further functionalization was achieved by coordination of gold to the phosphorus center, resulting in bathochromically shifted low energy absorption maxima and onsets.

■ EXPERIMENTAL SECTION

Materials and Measurements. Except where otherwise stated, reagents were purchased from Sigma-Aldrich and VWR and were used without any further purification. All reactions were performed under argon using flame-dried glassware and standard Schlenk techniques. THF and diethyl ether were dried over sodium benzophenone; DCM was dried over $CaCl_2$. All solvents were freshly distilled prior to use. Microwave reactions were carried out in a CEM Biotage Initiator reactor, and reaction temperature was monitored using the built-in IR sensor. Temperature profiles and durations are provided for the individual reactions. NMR spectra were recorded using a JEOL spectrometer (^{1}H frequency 400 MHz). High-resolution mass spectra were measured using FTMS + p APCI or FTMS + p NSI (OrbitrapXL) at the University of Münster. UV/vis spectra were recorded on a Varian Cary 50 or 50000 diodearray spectrophotometers.

X-ray Crystallography. All the measurements were performed using graphite-monochromatized Mo K_α radiation at 150 K using a Bruker D8 APEX-II equipped with a CCD camera. The structure was solved by direct methods (SHELXS-2014) and refined by full-matrix least-squares techniques against F^2 (SHELXL-2018).[47,48] The non-hydrogen atoms were refined with anisotropic displacement parameters. The H atoms of the CH_2 groups were refined with common isotropic displacement parameters for the H atoms of the same group and idealized geometry with approximately tetrahedral angles and C−H distances of 0.99 Å. The H atoms of the methyl groups were refined with common isotropic displacement parameters for the H atoms of the same group and idealized geometry with tetrahedral angles, enabling rotation around the X−C bond, and C−H distances of 0.98 Å. Additional details can be found in the cif files. Analysis of solid-state structures was carried out using Conquest.[49] Calculations are performed using the Gaussian suite of programs (G09 Rev D.01)[50] The structures are optimized at the DFT M06-2X level of theory using a 6-311G** basis set and the LANL2DZ pseudo

potential for Au. TD-DFT calculations are carried out using an extended basis set (6-311++G**/LANL2DZ). Among all tested functionals the best agreement with experimental UV/vis data was found for the PBE1PBE functional.

Synthesis of 2 and 3. Dibromo phosphaalkene **1** (108 mg, 0.18 mmol) and tributylstannylbenzothiophene (252 mg, 0.59 mmol, 3.2 equiv) were dissolved in 2 mL of THF (deaerated for 30 min) followed by addition of [Pd(PPh₃)₄] (22 mg, ~2% mol). The microwave tube was sealed under argon after degassing for 5 min, and then the vial was placed in the microwave reactor (CEM, Biotage) at 120 °C for 45 min. The crude reaction mixture was filtered through a thin pad of Celite (top) and silica (bottom) and concentrated under reduced pressure to yield a crude solid. The crude was dry-loaded into a column and eluted using a DCM:pentane gradient (1% to 10%) to yield **2** (R_f = 0.55, 5%) and **3** (R_f = 0.11, 5%) as a dark red solids. Single crystals of both compounds were obtained by slow evaporation of the solvents.

2: ^{1}H NMR (400 MHz, CDCl₃) δ 8.63 (d, J = 3.7 Hz, 1H), 7.89−7.85 (m, 1H), 7.82 (dd, J = 7.1, 1.1 Hz, 1H), 7.76−7.70 (m, 4H), 7.69−7.63 (m, 3H), 7.57 (d, J = 7.9 Hz, 1H), 7.38 (td, J = 7.5, 1.3 Hz, 1H), 7.33 (tt, J = 7.8, 1.5 Hz, 2H), 7.29 (dd, J = 7.7, 1.5 Hz, 1H), 7.17−7.10 (m, 1H), 6.46 (s, 1H), 1.50 (s, 18H), 1.41 (s, 9H). ^{13}C{^{1}H} NMR (101 MHz, CDCl₃) δ 154.1, 151.7, 144.9, 144.7, 140.9, 140.7, 139.5 (d, J = 14.4 Hz), 133.9, 133.3, 133.5, 133.3−133.0 (3−4 peaks), 128.8 (d, J = 5.2 Hz), 128.6 (d, J = 6.9 Hz), 127.2 (m, 2−3 peaks)126.6 (2d, ca. 5.9 Hz), 124.7 (m, min. 3 peaks), 124.4 (d, J = 6.0 Hz), 124.2, 123.6 (d, J = 7.0 Hz), 123.2 (2 peaks), 122.4, 122.1, 120.1 (2 peaks), 119.7 (2 peaks), 119.5, 118.4 (d, J = 24.5 Hz; maybe 2 peaks), 38.6, 35.4, 32.8 (d, J = 6.3 Hz), 31.5. (Several carbon resonances including the P═C could not be detected due to small quantities and insufficient resolution.) ^{31}P{^{1}H} NMR (162 MHz, CDCl₃) δ 268.4. HR-MS (APCI) m/z = M⁺ Calcd for C₄₇H₄₅PS₂ 704.2695; Found 704.2693; [M + H]⁺: Calcd for C₄₇H₄₆PS₂ 705.2773; Found 705.2727. Yield: 5 mg.

3: ^{1}H NMR (400 MHz, CDCl₃) δ 8.58 (d, J = 3.4 Hz, 1H), 7.85 (d, J = 7.8 Hz, 1H), 7.80 (d, J = 7.3 Hz, 1H), 7.69 (d, J = 8.5 Hz, 2H), 7.63 (s, 1H), 7.61 (s, 3H), 7.42 (d, J = 8.1 Hz, 1H), 7.37 (td, J = 7.5, 1.3 Hz, 1H), 7.32 (td, J = 7.5, 1.5 Hz, 1H), 7.28 (d, J = 8.2 Hz, 1H), 5.43 (s, 1H), 1.46 (s, 9H), 1.44 (s, 18H). ^{13}C{^{1}H} NMR (101 MHz, CDCl₃) δ 167.4 (d, 44.9 Hz), 154.2, 152.3, 144.6, 140.9, 139.6, 133.3 (d, J = 26.4 Hz), 131.0 (d, J = 5.9 Hz), 129.4 (d, J = 7.7 Hz), 127.2, 126.6 (2 peaks), 124.7, 124.4, 123.6, 123.1 (2 peaks), 122.4, 120.4 (2 peaks), 120.0, 119.6, 118.4, 118.2(2 peaks), 38.4, 35.4, 32.9 (d, J = 6.8 Hz), 31.6. ^{31}P{^{1}H} NMR (162 MHz, CDCl₃) δ 269.6. HR-MS (APCI) m/z = [M + H]⁺ Calcd for C₃₉H₄₁BrPS: 651.1845 and 653.183; Found 651.1835 and 653.1813; M⁺: Calcd for C₃₉H₄₀BrPS 650.1766 and 652.1752; Found 650.17686 and 652.17690 (Br isotope pattern). yield: 23 mg.

Synthesis of 5. Dibromo-phosphaalkene **1** (0.084 g, 1 equiv), [2,2′-bithiophen]-5-yltributylstannane **2** (0.1920 g, 3 equiv, [Pd-(PPh₃)₄], **3** (27 mg, 0.017 equiv ~17% mol), and THF (2 mL) were added to a dry microwave tube under argon. The solution was deaerated by thoroughly bubbling with argon for 45 min, and the capped tube was placed in a microwave reactor at 120 °C for 45 min. The crude reaction mixture was filtered through a thin pad of Celite (top) and silica (bottom) into a round-bottom flask using a glass-sintered frit and concentrated under reduced pressure to yield a crude solid. The crude was dry-loaded into a column and eluted using a 95:5 pentane:Et₂O mixture (R_f: 0.3) to yield **5** as a dark red solid. Single crystals were obtained from diffusion of a 1:1 pentane:Et₂O mixture into a vial of **5** dissolved in DCM (yield = 15.2 mg, 14%).

^{1}H NMR (400 MHz, THF-d8) δ 8.47 (d, J = 3.8 Hz = 1H), 7.70−7.61 (m, 5H), 7.45 (d, J = 3.8 Hz, 1H), 7.40 (dm, J = 8.1 Hz, 1H), 7.31 (ddd, J = 5.1, 2.6, 1.2 Hz, 2H), 7.28 (dd, J = 3.6, 1.2 Hz, 1H), 7.23 (d, J = 3.8 Hz, 1H), 7.18 (dd, J = 3.6, 1.2 Hz, 1H), 7.05−6.96 (m, 3H), 6.66 (d, J = 3.7 Hz, 1H), 6.35 (m, 1H), 1.48 (s 18H), 1.39 (s, 9H). ^{13}C{^{1}H} NMR (101 MHz, CDCl₃) δ 167.6 (d, J = 43.1 Hz), 154.3, 151.6, 144.3, 144.1, 143.8, 143.6, 139.6, 139.4, 138.5 (d, J = 9.7 Hz), 137.7, 137.4, 137.0, 136.9, 136.2, 133.6 (d, J = 58.0 Hz), 133.0, 132.5, 128.0 (d, J = 9.2 Hz), 126.5 (d, J = 5.4 Hz), 125.8 (d, J = 6.3

Hz), 124.7 (d, J = 7.9 Hz), 124.4 (d, J = 3.0 Hz), 123.9, 123.8, 123.7, 123.6, 123.2 (d, J = 7.5 Hz), 123.1, 120.0, 119.6, 117.6, 117.4, 38.6, 35.4, 32.7 (d, J = 6.4 Hz), 31.5. $^{31}P\{^1H\}$ NMR (162 MHz, THF-d8) δ 263.9. HR-MS (APCI) m/z = M$^+$ Calcd for $C_{47}H_{45}PS_4$ 768.2136; Found 768.2130; $[M + H]^+$: Calcd for $C_{47}H_{46}PS_4$ 769.2215; Found 769.2186. yield: 15.2 mg, 14%.

Characterization of 6.[29,51] ^1H NMR (400 MHz, CDCl$_3$) δ 8.50 (d, J = 4.2 Hz, 1H), 7.64 (s, 3H), 7.60 (d, J = 5.0 Hz, 1H), 7.59 (s, 1H), 7.47 (dd, J = 3.5, 1.3 Hz, 1H), 7.42(d, J = 8.1 Hz, 1H), 7.33 (dd, J = 5.1, 1.3 Hz, 1H), 7.29 (d, J = 8.2 Hz, 1H), 7.14 (dd, J = 5.1, 3.7 Hz, 1H), 5.47–5.42 (m, 1H), 1.50 (s, 9H), 1.47 (s, 18H). $^{13}C\{^1H\}$ NMR (101 MHz, CDCl$_3$) δ 167.7 (d, J = 44.1 Hz), 154.2 (d, J = 0.7 Hz), 152.3, 144.8, 143.5 (d, J = 26.5 Hz), 140.0 (d, J = 16.7 Hz), 137.7 (d, J = 10.3 Hz), 136.5 (d, J = 14.0 Hz), 133.7 (d, J = 2.7 Hz), 131.0 (d, J = 6.2 Hz), 129.4 (d, J = 7.5 Hz), 128.2, 126.2 (d, J = 6.6 Hz), 124.9, 123.4, 123.0, 120.7 (d, J = 4.2 Hz), 120.3 (d, J = 2.9 Hz), 120.0, 117.9 (d, J = 24.4 Hz), 38.4, 35.4, 32.9 (d, J = 6.8 Hz), 31.7. $^{31}P\{^1H\}$ NMR (162 MHz, CDCl$_3$) δ 268.4. HR-MS (APCI) m/z = M$^+$ Calcd for $C_{35}H_{38}BrPS$ 600.1610 and 602.1589; Found 600.1610 and 602.1579; $[M + H]^+$: Calcd for $C_{35}H_{39}BrPS$ 601.1688 and 603.1668; Found 601.1667 and 603.1643 (Br isotope pattern).

Synthesis of 7. Compound **1** (184 mg, 0.52 mmol) was added to 2-(Bu$_3$Sn)-pyridine (500 μL, 1.54 mmol) in 10 mL of THF, and the solution was degassed for 30 min. After adding $[Pd(PPh_3)_4]$ (130 mg, 0.1 mmol, 10 mol %) an immediate color change to dark blue occurred, and the sealed vial was placed in a microwave reactor for 45 min at 140 °C. The crude reaction mixture was passed through an alumina plug. Chromatographic workup (silica hexane/toluene) gave a relatively pure fraction of the mixed phosphine oxide phosphaalkene species. The splitting of the low frequency aromatic proton (6.36 ppm) indicates that the phosphine is in the sterically more shielded position, leading to a 3-bond P–H coupling ($^3J_{PH}$ = 11.0 Hz).

^1H NMR (400 MHz, CDCl$_3$) δ 9.51 (d, J = 3.2, 1H), 8.67 (d, J = 4.6 Hz, 1H), 8.27 (d, J = 8.2 Hz, 1H), 7.63 (2H), 7.55 (ps. tr., J = 7.8 Hz, 1H), 7.50–7.44 (m, 3H), 7.39 (1H), 7.35–7.27 (m, 4H), 7.14–7.08 (m, 4H), 6.99 (m, 1H), 6.70 (dd, J = 6.9 3.4 Hz, 1H), 6.36 (d, J = 11.0 Hz, 1H), 1.52 (9H), 1.49 (18H). $^{31}P\{^1H\}$ NMR (162 MHz, CDCl$_3$) δ 263.6 (P=C), –3.9 (–PPh$_2$) ppm. Satisfactory $^{13}C\{^1H\}$ data and other analysis could not be obtained.

In an attempt to identify how the diphenylphosphine transfer occurred, we reacted **1** (200 mg, 0.56 mmol) in the presence of excess PPh$_3$ (450 mg, 1.7 mmol) and $[Pd(PPh_3)_4]$ (150 mg, 0.13 mmol). The reaction solvent was THF, and the microwave was set to 165 °C for 90 min. The phosphine oxide was isolated in a mixture with OPPh$_3$. Diagnostic peaks in the phosphorus and proton NMR indicate the formation of the mixed phosphine phosphaalkene species **8**. Based on the absence of a substantial $^3J_{PH}$ coupling of the low frequency aromatic proton (br. s. 5.19 ppm), we assume that the coupling occurred at the less hindered position.

Selected NMR shifts: ^1H NMR (400 MHz, CDCl$_3$) δ 7.02 (d, J = 8.0 Hz, 1H), 6.61 (m, 2H), 6.44 (d, J = 7.9 Hz, 1H), 6.21 (ps. t, J = 7.8 Hz, 1H) 5.19 (br. s., 1H), 1.43 (9H), 1.35 (18H). $^{31}P\{^1H\}$ NMR (162 MHz, CDCl$_3$) δ 256.9 (P=C), 24.0 (–P(=O)Ph$_2$) ppm.

Synthesis of [AuCl*2]. A solution of **2** (11.65 mg, 0.0254 mmol) in 3 mL of DCM was mixed with 1 equiv of a $[AuCl(tht)]$ solution (8.14 mg), stirred for 2 h, and then filtered over Celite. The solvent was slowly evaporated, and all remaining volatiles were removed under reduced pressure. The product was collected as crystalline material in 96% yield.

^1H NMR (400 MHz, CDCl$_3$) δ 9.33 (d, J = 4.4 Hz, 1H), 7.95 (s, 1H), 7.04 (t, J = 13.3, 2H), 7.67–7.59 (m, 3H), 7.38–7.28 (m, 4H), 7.17 (s, 1H), 6.41 (d, J = 3.2 Hz, 1H), 1.67 (s, 18H), 1.40 (s, 9H). $^{13}C\{^1H\}$ NMR (101 MHz, CDCl$_3$) δ 158.6 (d, J = 79.0 Hz) 155.8, 155.5, 143.6, 142.9, 141.0, 140.5, 139.9, 139.6 (2 peaks), 139.4, 139.3, 139.2, 138.0, 137.8, 134.6, 134.6, 133.7, 133.7, 129.0–128.8 (d, 2 peaks), 125.4 (d, J = 9.6 Hz), 124.7, 124.7, 124.4 (d, J = 10.1 Hz), 124.3, 123.7, 122.2 (d, J = 19.3), 120.9, 120.6 (2 peaks), 119.8 (d, J = 21.0 Hz), 119.4, 39.6, 35.7, 34.3, 31.2 ppm. $^{31}P\{^1H\}$ NMR (162 MHz, CDCl$_3$) δ 181.4 ppm. HR-MS (MALDI) m/z = M + Au$^+$ Calcd for $C_{47}H_{45}PS_2Au_2Cl$ 1133.1715; Found 1133.1708.

Synthesis of [AuCl*3]. A solution of **3** (23.44 mg, 0.058 mmol) in 3 mL of DCM was mixed with 1 equiv of a $[AuCl(tht)]$ solution (18.7 mg), stirred for 2 h, and then filtered over Celite. The solvent was slowly evaporated, and all remaining volatiles were removed under reduced pressure. The product was collected as crystalline material in 98% yield.

^1H NMR (400 MHz, CDCl$_3$) δ 9.91 (d, J = 5.3 Hz, 1H), 7.94 (1H), 7.89 (d, J = 7.3 Hz, 1H), 7.84 (d, J = 7.8 Hz, 1H), 7.77 (d, J = 4.1 Hz, 2H), 7.75 (m, 1H), 7.59 (dd, J = 8.0, 18 Hz, 1H), 7.40–7.30 (m, 4H), 5.27 (d, J = 3.4 Hz, 1H), 1.62 (s, 18H), 1.46 (s, 9H). $^{13}C\{^1H\}$ NMR (101 MHz, CDCl$_3$) δ 158.8 (d, J = 80.1 Hz), 156.3, 142.7, 141.0, 140.5 (d, J = 13.6 Hz), 139.6, 139.0 (d, J = 5.8 Hz), 138.3, 138.0, 137.8, 137.6, 134.7 (d, J = 4.8 Hz), 133.1 (d, J = 7.7 Hz), 129.1 (d, J = 9.6 Hz), 128.9 (d, J = 7.7 Hz), 125.2 (d, J = 10.6 Hz), 124.7, 124.3, 122.3, 121.9 (d, J = 33.7 Hz), 123.3 (d, J = 6.7 Hz), 121.2 (d, J = 3.0 Hz), 121.0, 120.5, 119.7 (d, J = 20.2 Hz), 39.4, 35.8, 34.3, 31.3, 30.7. (Ortho and meta positions of the Mes* are not magnetically equivalent.) ^{31}P NMR (162 MHz, CDCl$_3$) δ 182.5 ppm. HR-MS (MALDI) m/z = M + Au$^+$ Calcd for $C_{39}H_{40}PBrSAu_2Cl$ 1081.0769; Found 1081.0757.

Synthesis of [AuCl*5]. A solution of **5** (7.15 mg, 0.0137 mmol) in 3 mL of DCM was mixed with 1 equiv of a $[AuCl(tht)]$ solution (8.14 mg), stirred for 2 h, and then filtered over Celite. The solvent was slowly evaporated, and all remaining volatiles were removed under reduced pressure. The product was collected as crystalline material in 82% yield.

^1H NMR (400 MHz, CDCl$_3$) δ 9.74 (d, J = 4.4 Hz, 1H), 7.79 (d, J = 3.9 Hz, 2H), 7.69 (m 1H), 7.58 (d, J = 8.0 Hz, 1H), 7.53 (d, J = 3.7 Hz, 1H) 7.51 (s, 1H), 7.44 (dm, J = 7.8 Hz, 1H), 7.27 (dd, J = 3.7 and 0.9 Hz, 1H), 7.24- 7.21 (m, 4H), 7.14 (dd, J = 3.4 and 0.9 Hz, 1H), 7.03 (ps. q, J = 4.9 Hz, 2H), 6.97 (d, J = 3.7 Hz, 1H), 6.54 (d, J = 3.9 Hz, 1H), 1.65 (s, 18H), 1.37 (s, 9H). $^{13}C\{^1H\}$ NMR (101 MHz, CDCl$_3$) δ 166.3 (d, J = 30 Hz), 156.1 (d, J = 79.0 Hz) 155.5, 142.7, 141.9, 139.9, 139.8, 139.5, 139.2, 138.7 (d, J = 17.3 Hz, 2C) 137.5, 137.3, 137.0 (d, J = 2.9 Hz) 134.2, 134.2, 133.2 (d, J = 5.8 Hz), 128.3 (d, J = 7.7 Hz), 128.0 (d, J = 9.6 Hz), 127.8 (d, J = 8.7 Hz), 125.3, 125.2 (d, J = 6.7 Hz), 124.8 (d, J = 7.7 Hz), 124.6 (d, J = 6.7 Hz), 124.1 (d, J = 7.7 Hz), 123.7, 123.0 (ps. m, 2C) 120.5, 119.0 (d, J = 21.2 Hz), 39.6, 35.7, 34.3, 31.2, 30.7. (Ortho and meta positions of the Mes* are not magnetically equivalent.) $^{31}P\{^1H\}$ NMR (162 MHz, CDCl$_3$) δ 179.6 ppm. HR-MS (MALDI) m/z = M + Au$^+$ Calcd for $C_{47}H_{44}PS_4Au_2Cl$ 1197.1156; Found 1197.1154.

■ ASSOCIATED CONTENT

ⓢ Supporting Information

The Supporting Information is available free of charge at https://pubs.acs.org/doi/10.1021/acs.joc.0c01336.

Experimental data (NMR spectroscopic and crystallographic data) (PDF)

NMR spectra of synthesized compounds and additional calculations (PDF)

CIF file (CIF)

■ AUTHOR INFORMATION

Corresponding Author

Andreas Orthaber − Synthetic Molecular Chemistry, Department of Chemistry − Ångström Laboratories, Uppsala University, 75120 Uppsala, Sweden; ⊙ orcid.org/0000-0001-5403-9902; Email: andreas.orthaber@kemi.uu.se

Authors

Joshua P. Green − Synthetic Molecular Chemistry, Department of Chemistry − Ångström Laboratories, Uppsala University, 75120 Uppsala, Sweden

Daniel Morales Salazar − Synthetic Molecular Chemistry, Department of Chemistry − Ångström Laboratories, Uppsala University, 75120 Uppsala, Sweden

Arvind Kumar Gupta − *Synthetic Molecular Chemistry, Department of Chemistry* − *Ångström Laboratories, Uppsala University, 75120 Uppsala, Sweden*

■ ACKNOWLEDGMENTS

■ REFERENCES

(1) Murphy, A. R.; Fréchet, J. M. J. Organic Semiconducting Oligomers for Use in Thin Film Transistors. *Chem. Rev.* **2007**, *107* (4), 1066−1096.

(2) Roncali, J. Synthetic Principles for Bandgap Control in Linear π-Conjugated Systems. *Chem. Rev.* **1997**, *97* (1), 173−206.

(3) Duan, L.; Qiao, J.; Sun, Y.; Qiu, Y. Strategies to Design Bipolar Small Molecules for OLEDs: Donor-Acceptor Structure and Non-Donor-Acceptor Structure. *Adv. Mater.* **2011**, *23* (9), 1137−1144.

(4) Shurdha, E.; Repasy, B. K.; Miller, H. A.; Dees, K.; Iacono, S. T.; Ball, D. W.; Balaich, G. J. Symmetrical bis(fulvene) chromophores: model compounds for acceptor−donor−acceptor dye architectures. *RSC Adv.* **2014**, *4* (79), 41989−41992.

(5) Lee, S. H.; Nakamura, T.; Tsutsui, T. Synthesis and Characterization of Oligo(9,9-dihexyl-2,7-fluorene ethynylene)s: For Application as Blue Light-Emitting Diode. *Org. Lett.* **2001**, *3* (13), 2005−2007.

(6) Liu, C.; Li, Y.; Li, Y.; Yang, C.; Wu, H.; Qin, J.; Cao, Y. Efficient Solution-Processed Deep-Blue Organic Light-Emitting Diodes Based on Multibranched Oligofluorenes with a Phosphine Oxide Center. *Chem. Mater.* **2013**, *25* (16), 3320−3327.

(7) Wu, H.-C.; Yu, A.-D.; Lee, W.-Y.; Liu, C.-L.; Chen, W.-C. A poly(fluorene-thiophene) donor with a tethered phenanthro[9,10-d]imidazole acceptor for flexible nonvolatile flash resistive memory devices. *Chem. Commun.* **2012**, *48* (73), 9135−9137.

(8) Thomas, K. R. J.; Kapoor, N.; Bolisetty, M. N. K. P.; Jou, J.-H.; Chen, Y.-L.; Jou, Y.-C. Pyrene-Fluorene Hybrids Containing Acetylene Linkage as Color-Tunable Emitting Materials for Organic Light-Emitting Diodes. *J. Org. Chem.* **2012**, *77* (8), 3921−3932.

(9) Muenmart, D.; Tarsang, R.; Jungsuttiwong, S.; Keawin, T.; Sudyoadsuk, T.; Promarak, V. Synthesis and properties of fluorene-oligothiophenes perylenediimide triads and their electropolymerizations. *J. Mater. Chem.* **2012**, *22* (29), 14579−14586.

(10) Duan, Z.; Hu, D.; Ohuchi, H.; Zhao, M.; Zhao, G.; Nishioka, Y. Organic field-effect transistors based on two phenylene−thiophene oligomer derivatives with a biphenyl or fluorene core. *Synth. Met.* **2012**, *162* (13−14), 1292−1298.

(11) Slodek, A.; Zych, D.; Maroń, A.; Golba, S.; Schab-Balcerzak, E.; Janeczek, H.; Siwy, M.; Maćkowski, S. Fluorene vs carbazole substituent at quinoline core toward organic electronics. *Dyes Pigm.* **2019**, *166*, 98−106.

(12) Tang, S.; Liu, M.; Lu, P.; Cheng, G.; Zeng, M.; Xie, Z.; Xu, H.; Wang, H.; Yang, B.; Ma, Y.; Yan, D. Fluorene trimers with various 9,9′-substituents: The synthesis, characteristics, condensed state structures, and electroluminescence properties. *Org. Electron.* **2008**, *9* (2), 241−252.

(13) Wang, X.; Hu, Y.-Z.; Chen, A.; Wu, Y.; Aggeler, R.; Low, Q.; Kang, H. C.; Gee, K. R. Water-soluble poly(2,7-dibenzosilole) as an ultra-bright fluorescent label for antibody-based flow cytometry. *Chem. Commun.* **2016**, *52* (21), 4022−4024.

(14) Hibner-Kulicka, P.; Joule, J. A.; Skalik, J.; Bałczewski, P. Recent studies of the synthesis, functionalization, optoelectronic properties and applications of dibenzophospholes. *RSC Adv.* **2017**, *7* (15), 9194−9236.

(15) Wu, B.; Yoshikai, N. Recent developments in synthetic methods for benzo[b]heteroles. *Org. Biomol. Chem.* **2016**, *14* (24), 5402−5416.

(16) Parke, S. M.; Boone, M. P.; Rivard, E. Marriage of heavy main group elements with π-conjugated materials for optoelectronic applications. *Chem. Commun.* **2016**, *52* (61), 9485−505.

(17) Green, J. P.; Wells, J. A. L.; Orthaber, A. Heavier pnictogens - treasures for optical electronic and reactivity tuning. *Dalton Trans.* **2019**, *48* (14), 4460−4466.

(18) Shameem, M. A.; Orthaber, A. Organophosphorus Compounds in Organic Electronics. *Chem. - Eur. J.* **2016**, *22* (31), 10718−10735.

(19) Nakahama, T.; Kitagawa, D.; Sotome, H.; Ito, S.; Miyasaka, H.; Kobatake, S. Optical properties and solvatofluorochromism of fluorene derivatives bearing S,S-dioxidized thiophene. *Photochem. Photobiol. Sci.* **2016**, *15* (10), 1254−1263.

(20) Mishra, A.; Ma, C.-Q.; Bäuerle, P. Functional Oligothiophenes: Molecular Design for Multidimensional Nanoarchitectures and Their Applications†. *Chem. Rev.* **2009**, *109* (3), 1141−1276.

(21) Kim, D.; Reddy, M. R.; Cho, K.; Ho, D.; Kim, C.; Seo, S. Solution-processable fluorene derivative for organic thin-film transistors. *Org. Electron.* **2020**, *76*, 105464.

(22) Kamtekar, K. T.; Vaughan, H. L.; Lyons, B. P.; Monkman, A. P.; Pandya, S. U.; Bryce, M. R. Synthesis and Spectroscopy of Poly(9,9-dioctylfluorene-2,7-diyl-co-2,8-dihexyldibenzothiophene-S,S-dioxide-3,7-diyl)s: Solution-Processable, Deep-Blue Emitters with a High Triplet Energy. *Macromolecules* **2010**, *43* (10), 4481−4488.

(23) Zuo, Z.; Ou, C.; Ding, Y.; Zhang, H.; Sun, S.; Xie, L.; Xia, R.; Huang, W. Spiro-substitution effect of terfluorenes on amplified spontaneous emission and lasing behaviors. *J. Mater. Chem. C* **2018**, *6* (16), 4501−4507.

(24) Vidal, F.; Jäkle, F. Functional Polymeric Materials Based on Main-Group Elements. *Angew. Chem., Int. Ed.* **2019**, *58* (18), 5846−5870.

(25) Deng, C.-L.; Bard, J. P.; Zakharov, L. N.; Johnson, D. W.; Haley, M. M. Naphtho[2,1-e]-1,2-azaphosphorine 2-Oxide Derivatives: Synthesis, Optoelectronic Properties, and Self-Dimerization Phenomena. *J. Org. Chem.* **2019**, *84* (12), 8131−8139.

(26) Belyaev, A.; Cheng, Y.-H.; Liu, Z.-Y.; Karttunen, A. J.; Chou, P.-T.; Koshevoy, I. O. A Facile Molecular Machine: Optically Triggered Counterion Migration by Charge Transfer of Linear Donor-π-Acceptor Phosphonium Fluorophores. *Angew. Chem., Int. Ed.* **2019**, *58* (38), 13456−13465.

(27) Hirai, M.; Tanaka, N.; Sakai, M.; Yamaguchi, S. Structurally Constrained Boron-, Nitrogen-, Silicon-, and Phosphorus-Centered Polycyclic π-Conjugated Systems. *Chem. Rev.* **2019**, *119* (14), 8291−8331.

(28) Baumgartner, T. Insights on the Design and Electron-Acceptor Properties of Conjugated Organophosphorus Materials. *Acc. Chem. Res.* **2014**, *47* (5), 1613−1622.

(29) Morales Salazar, D.; Mijangos, E.; Pullen, S.; Gao, M.; Orthaber, A. Functional small-molecules & polymers containing P= C and As = C bonds as hybrid π-conjugated materials. *Chem. Commun.* **2017**, *53* (6), 1120−1123.

(30) Svyaschenko, Y. V.; Orthaber, A.; Ott, S. Tuning the Electronic Properties of Acetylenic Fluorenes by Phosphaalkene Incorporation. *Chem. - Eur. J.* **2016**, *22* (12), 4247−4255.

(31) Van der Knaap, T. A.; Bickelhaupt, F. (2,6-Dimethylphenyl)(9-fluorenyliden)Phosphan. *Chem. Ber.* **1984**, *117* (3), 915−924.

(32) Typical procedures attempted to combine **1** and the thienyl boronic acid using K_2CO_3 (or Cs_2CO_3) and a solvent (MeOH or MeOH/water, THF, MeOH) at room temperature or at elevated temperatures (60 °C).

(33) Lee, Y. H.; Morandi, B. Transition metal-mediated metathesis between P−C and M−C bonds: Beyond a side reaction. *Coord. Chem. Rev.* **2019**, *386*, 96−118.

(34) Kwong, F. Y.; Lai, C. W.; Tian, Y.; Chan, K. S. A novel synthesis of functionalised tertiary phosphines by palladium catalysed phosphination with triarylphosphines. *Tetrahedron Lett.* **2000**, *41* (52), 10285−10289.

(35) Le Floch, P.; Carmichael, D.; Ricard, L.; Mathey, F. Palladium(0)-catalyzed functionalization of bromophosphinines. *J. Am. Chem. Soc.* **1993**, *115* (23), 10665−10670.

(36) Fraysse, S.; Coudret, C. Unexpected formation of a scrambled aryl-phosphine oxide under modified sonogashira conditions. *Tetrahedron Lett.* **1999**, *40* (52), 9249−9250.

(37) Van der Knaap, T. A.; Jenneskens, L. W.; Meeuwissen, H. J.; Bickelhaupt, F.; Walther, D.; Dinjus, E.; Uhlig, E.; Spek, A. L. Complex formation between nickel(0) and a phosphaalkene: influence of the second ligand on the η^1- and η^2-coordination mode. *J. Organomet. Chem.* **1983**, *254*, C33−C36.

(38) Öberg, E.; Orthaber, A.; Lescop, C.; Réau, R.; Hissler, M.; Ott, S. Phosphorus Centers of Different Hybridization in Phosphaalkene-Substituted Phospholes. *Chem. - Eur. J.* **2014**, *20* (27), 8421−8432.

(39) Ito, S.; Zhai, L.; Mikami, K. Combination of sp²- and sp³-Type Phosphorus Atoms for Gold Chemistry: Preparation, Structure, and Catalytic Activity of Gold Complexes That Bear Ligated 2-Silyl-1,3-diphosphapropenes. *Chem. - Asian J.* **2011**, *6* (11), 3077−3083.

(40) Miesel, D.; Korb, M.; Hildebrandt, A.; Lang, H. Synthesis and crystal structure of an acetylenic ferrocenyl substituted phosphaalkene. *Inorg. Chim. Acta* **2018**, *471*, 741−745.

(41) Rawe, B. W.; Brown, C. M.; MacKinnon, M. R.; Patrick, B. O.; Bodwell, G. J.; Gates, D. P. A C-Pyrenyl Poly(methylenephosphine): Oxidation "Turns On" Blue Photoluminescence in Solution and the Solid State. *Organometallics* **2017**, *36* (14), 2520−2526.

(42) Nauroozi, D.; Orthaber, A. The Heavier Analogues of Alkenes: A Theoretical Comparison of Unsaturated Group 15/14 Systems. *Eur. J. Inorg. Chem.* **2016**, *2016* (5), 709−717.

(43) The second disordered molecule shows very similar metrics and is not discussed herein.

(44) Seven phosphaalkene gold chloride complexes have been structurally characterized. mean P=C, P−Au distances and C−P=C angles are 1.682 Å, 2.217 Å, and 110.7°.

(45) Orthaber, A.; Löfås, H.; Öberg, E.; Grigoriev, A.; Wallner, A.; Jafri, S. H. M.; Santoni, M.-P.; Ahuja, R.; Leifer, K.; Ottosson, H.; Ott, S. Cooperative Gold Nanoparticle Stabilization by Acetylenic Phosphaalkenes. *Angew. Chem., Int. Ed.* **2015**, *54* (36), 10634−10638.

(46) Freytag, M.; Ito, S.; Yoshifuji, M. Coordination Behavior of Sterically Protected Phosphaalkenes on the AuCl Moiety Leading to Catalytic 1,6-Enyne Cycloisomerization. *Chem. - Asian J.* **2006**, *1* (5), 693−700.

(47) Sheldrick, G. Crystal structure refinement with SHELXL. *Acta Crystallogr., Sect. C: Struct. Chem.* **2015**, *71* (1), 3−8.

(48) Dolomanov, O. V.; Bourhis, L. J.; Gildea, R. J.; Howard, J. A. K.; Puschmann, H. OLEX2: a complete structure solution, refinement and analysis program. *J. Appl. Crystallogr.* **2009**, *42* (2), 339−341.

(49) Bruno, I. J.; Cole, J. C.; Edgington, P. R.; Kessler, M.; Macrae, C. F.; McCabe, P.; Pearson, J.; Taylor, R. New software for searching the Cambridge Structural Database and visualizing crystal structures. *Acta Crystallogr., Sect. B: Struct. Sci.* **2002**, *58* (3), 389−397.

(50) Frisch, M. J.; Trucks, G. W.; Schlegel, H. B.; Scuseria, G. E.; Robb, M. A.; Cheeseman, J. R.; Scalmani, G.; Barone, V.; Mennucci, B.; Petersson, G. A.; Nakatsuji, H.; Caricato, M.; Li, X.; Hratchian, H. P.; Izmaylov, A. F.; Bloino, J.; Zheng, G.; Sonnenberg, J. L.; Hada, M.; Ehara, M.; Toyota, K.; Fukuda, R.; Hasegawa, J.; Ishida, M.; Nakajima, T.; Honda, Y.; Kitao, O.; Nakai, H.; Vreven, T. J. A.; Montgomery, J.; Peralta, J. E.; Ogliaro, F.; Bearpark, M.; Heyd, J. J.; Brothers, E.; Kudin, K. N.; Staroverov, V. N.; Keith, T.; Kobayashi, R.; Normand, J.; Raghavachari, K.; Rendell, A.; Burant, J. C.; Iyengar, S. S.; Tomasi, J.; Cossi, M.; Rega, N.; Millam, J. M.; Klene, M.; Knox, J. E.; Cross, J. B.; Bakken, V.; Adamo, C.; Jaramillo, J.; Gomperts, R.; Stratmann, R. E.; Yazyev, O.; Austin, A. J.; Cammi, R.; Pomelli, C.; Ochterski, J. W.; Martin, R. L.; Morokuma, K.; Zakrzewski, V. G.; Voth, G. A.; Salvador, P.; Dannenberg, J. J.; Dapprich, S.; Daniels, A. D.; Farkas, O.; Foresman, J. B.; Ortiz, J. V.; Cioslowski, J.; Fox, D. J. *Gaussian 09*, Revision D.01; Gaussian Inc.: Wallingford, CT, 2013.

(51) Compound **6** is isolated from the attempted synthesis of the disubstituted derivative as described in ref 29.